

Nucleation Rates in a New Phenomenological Model[†]Roya Zandi,^{*,‡,§} David Reguera,^{||} and Howard Reiss[‡]

Department of Chemistry and Biochemistry, University of California at Los Angeles, Los Angeles, California 90095-1569, and Departament de Física Fonamental, Facultat de Física, Universitat de Barcelona, Martí i Franquès 1, Barcelona 08028, Spain

Received: December 20, 2005; In Final Form: March 12, 2006

In this paper we develop a new theory to evaluate the nucleation rate in the framework of the EMLD-DNT model. Beyond the model, our theory deals with cluster translation and exclusion, effects that have been virtually ignored in classical nucleation theory. We apply the model to the case of 1-pentanol, and compare the predictions with experimental results. We find an excellent agreement between the nucleation rate predicted by our theory and experimental data. The distinguishing feature of the model is its ability to predict successfully the rate of formation of the critical nucleus without the use of an intermolecular potential, employing only macroscopic thermodynamic properties.

1. Introduction

Nucleation is the process governing many phase transformations, and as such, it has an enormous impact in several fields ranging from atmospheric science through condensed matter phenomena to biological systems.^{1,2} Despite its great importance, it is still an open field. Classical nucleation theory (CNT) has been used extensively to predict nucleation rates in terms of macroscopic measurable quantities. However, during the past decade many experimental investigations have shown that the predictions of CNT are in severe disagreement with experiments. Accordingly, development of new theories and, in particular, new phenomenological theories predicting nucleation rates based on macroscopic thermodynamic parameters are highly desirable and are intensively investigated.^{3–10}

In a recent series of papers,^{11–13} a theory of cluster formation, namely, the *extended modified liquid drop* (EMLD) model, was developed and applied in the quantitative evaluation of various properties of argon clusters. The theory is distinguished by the fact that it requires as input only the values of macroscopic thermophysical observables. Yet, for the case of argon, it was able to predict, with remarkable accuracy, the values of these cluster properties evaluated by Monte Carlo (MC) simulation based on the known argon intermolecular potential. Unfortunately, at this time, there are no reliable experimental data on such argon cluster properties, thus leaving simulation as the substitute for experiment.

More recently, EMLD has been combined with *dynamical nucleation theory* (DNT)¹⁴ based, among other things, on *variational transition state theory* (VTST),¹⁵ to generate a theory (EMLD-DNT)^{16,17} for the evaluation of quantities of importance to the theory of nucleation in the condensation of supersaturated vapors. Again, in the case of argon, remarkable agreement between theory and simulation^{16,17} was obtained. For example, the free energy barrier opposing nucleation was accurately predicted and, in addition, for a finite value of supersaturation,

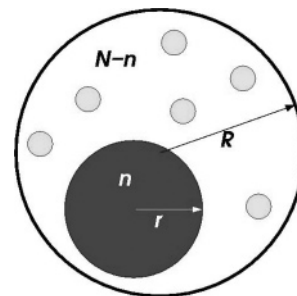


Figure 1. Schematic illustration of the system considered in the EMLD model. The total number of particles N inside the box is shared between a liquid drop of radius r containing n particles and the remaining $N-n$ molecules of the vapor phase. The volume of the spherical container is $V = 4\pi R^3/3$.

the vanishing of the nucleation barrier was demonstrated, thus resembling the existence of a spinodal. However, it was still not possible to use EMLD-DNT to predict a nucleation *rate*. In the present paper EMLD-DNT is revisited in order to develop a theory of *rate* and to apply it to the nucleation of 1-pentanol, a substance for which abundant experimental data exist on the nucleation of its supersaturated vapor.^{18–20}

Before proceeding to the main sections of this paper it is useful to provide the reader with brief descriptions of EMLD and EMLD-DNT.

2. EMLD and EMLD-DNT

The EMLD theory models the behavior of a system consisting of N molecules enclosed in a rigid spherical shell of volume V and radius R , at a fixed temperature T .¹¹ The N molecules are distributed between an incompressible spherical drop of n molecules and radius r , and the surrounding vapor of $N-n$ molecules. Usually the vapor is considered to be ideal and the drop has the uniform density of the bulk liquid as well as a sharp interface with the vapor. The interface is assumed to exhibit the surface tension of the plane surface of a bulk liquid. The center of the rigid drop may be positioned anywhere within a spherical volume of radius $R-r$, i.e., it is allowed to translate in the spherical container. Figure 1 is helpful in visualizing this system.

[†] Part of the special issue "Charles M. Knobler Festschrift".

[‡] University of California at Los Angeles.

[§] Present address: Department of Physics, University of California at Riverside, Riverside, CA 92521. E-mail: Roya.Zandi@ucr.edu.

^{||} Universitat de Barcelona.

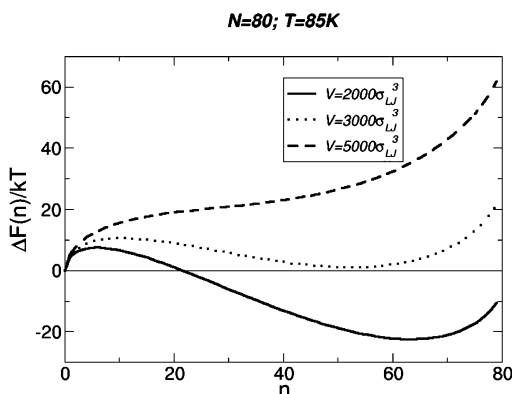


Figure 2. Free energy, eq 1, as a function of the size of the cluster for $N = 80$ molecules of Lennard-Jones argon at $T = 85$ K, and three different values of the volume expressed in Lennard-Jones units, σ .

If the free energy of translation is discounted, a straightforward thermodynamic analysis¹¹ shows that, as a function of n , the Helmholtz free energy of formation $\Delta F(n)$ of the cluster from an initially uniform ideal gas of N molecules within V , is

$$\Delta F(n) = -nkT \ln(P_1/P_1^{\text{eq}}) + \sigma A + n(kT - v_l P_1^{\text{eq}}) + NkT \ln(P_1/P_0) \quad (1)$$

where k is the Boltzmann constant, T is the temperature, $P_1 = (N - n)kT/(V - v_l n)$ is the pressure exerted by the ideal gas, P_1^{eq} is the vapor pressure of the bulk liquid, σ is the (planar) surface tension, A is the surface area of the spherical drop of radius r containing n molecules, v_l is the volume per molecule in the liquid, and $P_0 = NkT/V$. For argon, plots of $\Delta F(n)$ versus n for several values of V appear in Figure 2.

The plots are S-shaped, indicating both a maximum and minimum of $\Delta F(n)$ as a function of n . It may be demonstrated that the vapor pressure of the drop of size $n = n_{\text{min}}$, corresponding to the minimum, satisfies the Kelvin relation;¹¹ i.e., p_1 is the equilibrium vapor pressure of a drop of size n_{min} . However, on the free energy landscape represented by a curve in Figure 2, the drop is not constrained to the size n_{min} , and n may fluctuate over the landscape with a thermodynamic probability proportional to $\exp\{-\Delta F(n)/kT\}$. Therefore the thermodynamic properties of the cluster, e.g., the internal pressure exerted on the shell, are not those characterized by n_{min} alone but by an average over n weighted by $\exp\{-\Delta F(n)/kT\}$. However, this is not the full story because, within V , eq 1 neglects the translational free energy of the drop. In EMLD this contribution is accounted for by regarding the drop as a single hard molecule of ideal gas that exerts the partial pressure $p_r = 3kT/4\pi(R - r)^3$ on the interior of the shell. However, this quantity must also be averaged over the fluctuation of r or n . There is some subtlety associated with the inclusion of the translational contribution in this manner^{11,13} and the reader is referred to ref 13 for further detail. The full pressure exerted on the shell is then the weighted average of $P_1 + p_r$; i.e., $P = \langle P_1 + p_r \rangle$.

The hallmark of EMLD is the inclusion, in the model, of fluctuations over n . Such fluctuations are of negligible importance for a system in the thermodynamic limit but are quite important for a small system such as an EMLD cluster. Clearly, when the minimum in Figure 2 is very deep (for example, at small V), the thermodynamic properties of the cluster will be dominated by $n = n_{\text{min}}$, but as V is increased, this becomes less true. At large enough V , $\Delta F(n_{\text{min}})$ at the minimum exceeds $\Delta F(0) = 0$ (which corresponds to the presence of only a vapor

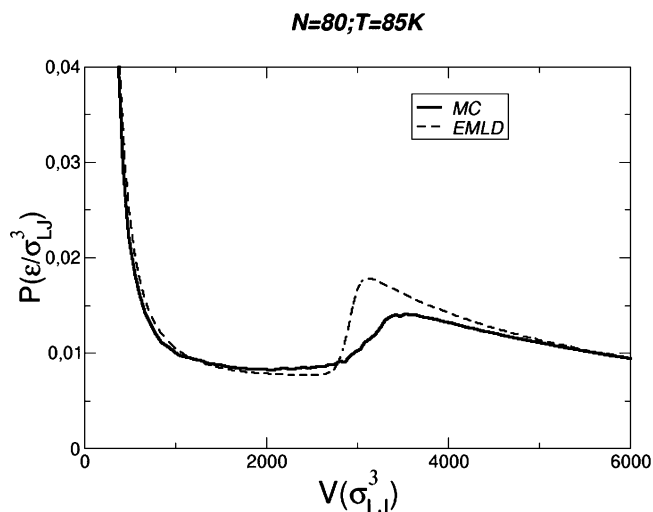
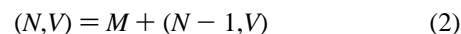


Figure 3. Value of the pressure vs volume isotherm for $N = 80$ molecules of argon at $T = 85$ K. The dashed line represents the prediction of the EMLD model, and the solid line, the results of MC simulation.

within V) so that the system at n_{min} would be metastable. At still larger V the free energy landscape loses its S-shaped character; i.e., the minimum disappears, and only an ideal gas remains within the shell.¹¹

The pressure–volume (P – V) isotherm of the “cluster” can be derived from $\Delta F(n)$, and an example, for argon, is presented in Figure 3. For comparison, the same isotherm evaluated via MC simulation is included in the figure. The excellent agreement between the two curves, even though the EMLD curve is obtained without the use of an intermolecular potential, should be noted.

The *total* construct involving both drop and vapor can be defined as an N, V -cluster. The accounting of fluctuations and translation makes the density profile of this cluster smooth (see ref 11), and thus it becomes a good candidate to replace and overcome the limitations of the capillarity cluster of classical nucleation theory. However, an important problem remains. The N, V -cluster is described by *both* N and V and the question arises: “Given N , what is the corresponding V ?” In other words, for the defined EMLD cluster what is the function $V(N)$? Here is where DNT shows its value and leads to the composite theory EMLD-DNT. DNT provides a criterion for selecting the volume of the cluster based on the kinetics of the process and more specifically on variational transition state theory (VTST). In DNT, the evaporation of a single molecule from an N, V -cluster is seen as a “chemical reaction”. The reaction can be represented by



where M is the stoichiometric formula for a single vapor molecule and the entities in parentheses are the formulas for clusters of size N and $N - 1$, respectively. In VTST,^{14,15} one defines a “reaction surface” in phase space such that all states of the system on one side of the surface correspond to products while states on the other side belong to reactants. In our case, the relevant reaction surface should be an abstract sphere coinciding with the spherical shell of the cluster. The variational feature of the theory consists of varying the position and shape of the surface so as to minimize the reactant flux crossing it. The corresponding flux then provides an upper bound to the true reaction rate. It was shown that the minimum evaporative flux can be associated with the V corresponding to the minimum

value of P on the isotherm. Then the spherical surface corresponding to this value of volume V can be chosen as the EMLD-DNT volume of the shell going with N .

Suppose that we wish to use an EMLD-DNT cluster in a theory of homogeneous vapor phase nucleation. Then, in a supersaturated vapor of pressure P , the cluster corresponding to the condensation nucleus will be the one whose pressure is P , since the nucleus must be in unstable equilibrium with the surrounding vapor. Knowing N , one can generate the P – V isotherm of the cluster and, from the pressure minimum, determine the appropriate V . Using eq 1 together with other relations elaborated below, one can evaluate ΔG^* , the Gibbs free energy of formation of the critical cluster, and therefore the height of the free energy barrier opposing nucleation.

This program has actually been implemented for the nucleation of supersaturated argon vapor.^{16,17} The calculated barriers are in excellent agreement with those evaluated via MC simulation.²¹ Furthermore, the existence of a spinodal, i.e., a finite value of the supersaturation at which the nucleation barrier vanishes, can be implied.^{16,17} All of this has been achieved without the use of an intermolecular potential. Thus, a successful application of these ideas to one aspect of nucleation theory has been already achieved.

However, only a theory for the barrier height has been developed. It remains to formulate a quantitative theory for the nucleation rate itself. We address this problem in the following sections.

3. The Ensemble Problem

The original EMLD theory has been developed within a *closed* small canonical or N, V, T ensemble. However, real nucleation normally occurs within a supersaturated vapor in which growing clusters are *open* systems that freely accumulate molecules from the surrounding vapor phase. Consequently the μ, V, T or grand ensemble is the natural vehicle within such a theory should be formulated. Therefore, if EMLD clusters are to be used in a theory of the nucleation rate, a connection, suitable to the nucleation process, between the canonical and grand ensembles must be constructed.

Fortunately such a connection is already available.¹⁶ The following relations have been proved, first by Lee, Telo de Gamma, and Gubbins²² and elaborated by Reguera and Reiss¹⁶

$$(\Delta\Omega)_{\mu^*, V, T} = (\Delta G)_{N^*, P^*, T} = (\Delta F)_{N^*, V, T} + N^*(\mu_0 - \mu^*) - V(P_0 - P^*) \quad (3)$$

Equation 3 is strictly valid only for a condensation nucleus, i.e., when N^* represents the size of a nucleus (in unstable equilibrium with the surrounding supersaturated vapor). In eq 3, Ω represents the grand potential of the cluster, G represents the Gibbs free energy, and F the Helmholtz free energy. The Δ values indicate changes in the respective thermodynamic potentials that accompany the formation of the nucleus, i.e., reversible works of formation. Equation 3 contains a number of subtleties that merit further discussion. Not only are the initial states of the various processes, whose works are related by the equation, different but also processes in *closed* and *open* systems are related. There is nothing at fault with these situations. One merely has to understand that the right side of the equation, no matter how different in composition and restriction, is an exact *measure* of the quantities on the left, as has been proved by rigorous thermodynamic analysis.²² A particular derivation of eq 3 is given in Appendix A.

In eq 3, μ_0 is the chemical potential of the uniform initial vapor in the ΔF process, and if that vapor is ideal, it follows that $\mu_0 = \mu_{\text{eq}} + kT \ln(P_0/P_{\text{eq}})$ where μ_{eq} is the chemical potential, at T , of the saturated vapor, and P_{eq} is its pressure. Again, μ^* and P^* in the equation are the chemical potential and pressure of the supersaturated vapor while N^* and V are the total number of molecules and volume of the nucleus. If the nucleus is modeled as an EMLD-DNT cluster, the radial distribution of density within it is determined by both the weighted average of n due to fluctuations and by the random average over the allowed positions of the corresponding “drop”.¹¹ It should also be mentioned that $(\Delta F)_{N^*, V, T}$ in eq 3 is prescribed by¹¹

$$(\Delta F)_{N^*, V, T} = -kT \ln \sum_{n=0}^{N^*} \exp(-\Delta F(n)/kT) \quad (4)$$

Equation 3 represents the work of formation of the critical cluster or nucleus, which is one of the key quantities in the process of nucleation. The other relevant quantity is the size of the nucleus. In this context, one has to bear in mind that the EMLD-DNT clusters contain a significant amount of vapor. It is thus important to clarify that N^* is the *total* number of molecules in the cluster, but it does not represent the actual physically meaningful quantity of a nucleating drop, which is the molecular *excess*. This excess can be properly defined as the number of molecules that the drop contains in excess of that due to the uniform vapor phase. This excess ΔN^* can be obtained through the use of the nucleation theorem^{23,24}

$$\Delta N^* = - \frac{\partial(\Delta G^*)_{N^*, P^*, T}}{\partial \Delta \mu} \Big|_{V, T} \quad (5)$$

It was shown, for the case of argon, that this excess coincides with the critical cluster (drops) size predicted by CNT and measured in MC simulations.²¹

4. Growth Path to the EMLD-DNT Nucleus

As already indicated, EMLD clusters, restricted only by their original definition are functions of both N and V . The additional requirement that the cluster also satisfy DNT renders V a function of N so that the EMLD-DNT cluster depends only on N . The nucleation process involves the growth of a cluster, i.e., the increase of N toward the nucleus size N^* . If the growing cluster was, at most, of the EMLD variety, there would be an infinite number of possible growth paths on a two-dimensional N, V surface. Of course, if every cluster on the growth path was an EMLD-DNT cluster, there would be only *one* path, since V would be a function of N . However, one has to bear in mind that the actual physical cluster is an open system that grows in a grand ensemble environment, i.e., in a reservoir of supersaturated vapor in which both μ and accordingly P and V are constant. At the same time, the pressure of an EMLD-DNT cluster must vary with N . This follows from the fact that $V(N)$ is determined by VTST as the volume that minimizes the reactant flux in eq 2 and that the operational approach to making this choice involves finding the V that minimizes the pressure on the P – V isotherm belonging to the cluster of size N . The pressure going with that minimum varies with N . As a result, if the growth path consists of DNT clusters, it cannot be one of constant P . Therefore, although the nucleus is a DNT cluster, the fact that clusters smaller than the nucleus, on the growth path, must have the same P means that they cannot be DNT clusters. Furthermore, they cannot be in equilibrium with the surrounding vapor, so that eq 3 cannot, in principle, be used in

the rigorous evaluation of their properties. However, the situation is saved by a thermodynamic expression that provides us with the work of formation of our N,V -clusters at the pressure (or supersaturation) of interest. This expression relies on the reasonable assumption²⁵ (partially justified by analysis²⁵) that the free energy of a cluster is determined primarily by its internal structure. On the basis of this assumption, Talanquer and Oxtoby²⁶ were able to derive the following relation

$$(\Delta\Omega)_{\mu,V,T} = (\Delta\Omega^*)_{\mu^*,V,T} + N^*(\mu^* - \mu) - V(P^* - P) + \Delta F^{\text{int}} \quad (6)$$

This is essentially eq 25 of ref 26, but the notation has been changed to suit our present needs. For example the asterisk indicates that the final state of the change indicated by Δ is that of the condensation nucleus corresponding to a supersaturated vapor of pressure P^* and chemical potential μ^* . The reversible work of formation of the cluster of primary interest is represented by $(\Delta\Omega)_{\mu,V,T}$. The cluster is *not* in equilibrium with the surrounding vapor whose pressure is P and whose chemical potential is μ . The reader should find it helpful to read the derivation of Talanquer and Oxtoby.²⁶ The approximation that the cluster free energy is determined only by its internal structure amounts to setting equal to zero ΔF^{int} which, in eq 6, represents the interaction free energy between the nonequilibrium cluster and its surroundings. Note that in case of an ideal gas, ΔF^{int} is very approximately equal to zero. Then, setting ΔF^{int} , in eq 6, equal to zero and inserting eq 3, leads to

$$(\Delta\Omega)_{\mu,V,T} = (\Delta F)_{N^*,V,T} + N^*(\mu_0 - \mu) - V(P_0 - P) \quad (7)$$

The approximation in question is chiefly the assumption that $(\Delta F)_{N^*,V,T}$, corresponding to the cluster formed in a vapor of pressure P , is the same as the ΔF when the cluster is formed in a vapor at the equilibrium pressure P^* ; i.e., its free energy is determined mainly by its internal structure. Talanquer and Oxtoby used eq 6 as a simple means of evaluating the work of cluster formation in a vapor of arbitrary supersaturation, once the work had been calculated for a “reference” vapor at pressure P^* . Equation 7 then determines the landscape for the free energy of formation of EMLD-DNT clusters.

The question remains as to what is the growth path on this landscape?

In principle, without further consideration, the path on the N,V surface is completely arbitrary, save for the fact that it must lead to the chosen nucleus.

However, there is a further consideration associated with the fact that EMLD clusters of the same N , but having different V values, are not statistically independent. This follows from the fact that in the case of two clusters, one characterized by N,V_2 and the other by N,V_1 , where $V_2 > V_1$, the cluster with the larger volume can realize all of the molecular configurations of the smaller cluster in addition to configurations not realizable by the one having the smaller volume. A particular example of this sort of unallowable redundancy is discussed in the following section on translation. The avoidance of such redundancy therefore requires a growth path (increase of N) on the free energy landscape that contains no change of V . The relevant constant V must therefore be the V^* of the nucleus, and the “vertical” path on the N,V surface must be the correct one.

Along this path, the nucleus is the only DNT cluster and its V and P , the volume and pressure of the supersaturated vapor, are the V and P of the path. The full set of variables for a cluster must then be N,P,V,T , and the growth path (increase of N or equivalently ΔN) on the landscape is fully defined by P,V,T .

Furthermore, along the growth path of *both* constant V and constant P , we can prove that

$$\left[\frac{\partial \Delta G}{\partial N} \right]_{P,V,T} \Big|_{N=N^*} = 0$$

which is the condition for an extremum (maximum) for ΔG .

To this end, we start with differentiating eq 3 with respect to N

$$\left[\frac{\partial \Delta G}{\partial N} \right]_{P,V,T} = \left[\frac{\partial \Delta F}{\partial N} \right]_{P,V,T} \Big|_{N=N^*} + (\mu_0 - \mu^*) + N \left[\frac{\partial(\mu_0 - \mu^*)}{\partial N} \right]_{P,V,T} - V \left[\frac{\partial(P_0 - P^*)}{\partial N} \right]_{P,V,T}$$

Note that μ^* and P^* are the externally imposed values of the chemical potential and pressure and are thus constant. Since μ_0 and P_0 are related to the chemical potential and pressure of a uniform vapor system, according to the Gibbs–Duhem relation, the last two terms of the above equation cancel each other. Interestingly enough, the first term on the right-hand side is just the definition of the difference in chemical potentials between initial and final states

$$\left[\frac{\partial \Delta F}{\partial N} \right]_{V,T} = \mu^* - \mu_0.$$

Thus $[\partial \Delta G / \partial N]_{P,V,T}$ is identically equal to zero, which confirms that ΔG goes through a maximum at the critical nucleus on the constant V and constant P path.

In the following sections we develop a theory for the rate of nucleation along this path.

5. Translation

According to eq 3, the reversible work of cluster formation $(\Delta\Omega)_{\mu,V,T}$ can be represented by $(\Delta G)_{N^*,P,T}$. For the purpose of manipulation, it is somewhat more convenient to represent the work by ΔG than by $\Delta\Omega$, and we shall follow this procedure. We shall also drop the asterisk on N . The work on the “growth path” can now be represented by $(\Delta G)_{N,P,V,T}$ since, in accordance with the preceding section, V as well as P is constant along that path. However, we must now deal with the frequently unrecognized fact that $(\Delta G)_{N,P,V,T}$ used in the preceding analysis does not contain the full translational free energy of the cluster within the ambient supersaturated vapor. For the correct derivation of the nucleation rate the additional translational free energy should be included. The most direct path to this value involves the derivation of the additional factor that it generates in the cluster canonical ensemble partition function. We perform this derivation in the present section.

Figure 4 will be used in the analysis. It shows a cluster consisting of say N molecules confined within a rigid spherical container of volume V . Clearly, the EMLD cluster belongs to this class. The cluster is shown in two infinitesimally separated positions. In the initial position, the cluster’s spherical boundary is a full line. In a displaced position, the boundary is dashed. The centers of the spherical container in the two positions are depicted as two black dots. The infinitesimal displacement is shown as dz . The five filled circles represent the N molecules within the cluster. Notice that the molecules belong to both the initial and displaced cluster, since they are located in the lens-shaped volume of overlap. The volume of the cluster is V . The total number of molecules in the system is denoted by N_{tot} , and the total volume of the system is denoted by V_{tot} . Thus, the volume outside of the cluster is $V_{\text{tot}} - V$ and the number of

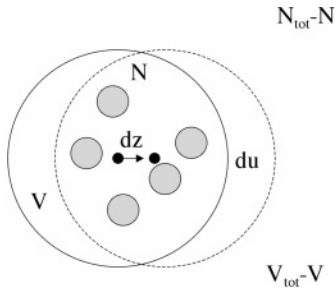


Figure 4. (a) Drop of volume V , containing N molecules (filled circles), embedded in an ideal gas of volume $V_{\text{tot}} - V$, and consisting of $N_{\text{tot}} - N$ molecules. The cluster in the initial position is the large continuous circle. Cluster with center displaced by dz is the dashed circle. Drop molecules are in the lens-shaped region created by the overlap of the original and displaced profiles. Nonoverlapped volume is denoted by du .

molecules outside is $N_{\text{tot}} - N$. The nonoverlapped cluster volume is shown as du .

It is important to note that the configuration integral of the cluster is an integral including all configurations of its *molecules*. Thus the configurations in the lens-shaped volume of overlap belong to both the initial and displaced clusters and the displacement has not moved the *physical* cluster if all the molecules in both cases lie in the lens-shaped region. Thus, care must be taken to avoid redundancy in the evaluation of the configuration integral of the system consisting of the initial plus the displaced cluster.

The full partition function of the N -cluster in the volume V_{tot} will be denoted by $Q_N(V_{\text{tot}})$. This partition function contains a translational factor which, if omitted, leaves the partition function $q(N)$ of the stationary cluster we have been treating in the above analysis. For consistency we can denote this partition function as

$$q(N) = q(N, V, T, P) = \exp\{-F(N, V, T, P)/kT\} \quad (8)$$

and what we need is

$$Q_N(V_{\text{tot}}) = \Phi_N(V_{\text{tot}})q(N, V, T, P) \quad (9)$$

where $\Phi_N(V_{\text{tot}})$ is the additional translational factor. We now have to evaluate $\Phi_N(V_{\text{tot}})$. Figure 4 will be helpful in this process.

We proceed by allowing the cluster to assume additional positions, i.e., we allow the center of the spherical shell (not necessarily the center of mass) to move. The figure illustrates a situation in which the center of the drop has been displaced from the initial position by the vector distance dz . Again, an important conclusion to be gleaned from the figure is that the movement of the shell does not necessarily lead to *molecular* configurations that were not possible in the initial position. Thus a new *physical* state may not be generated by the displacement. To have a new physical state there would have to be *at least* one molecule in the nonoverlapped volume designated as du .

To represent the augmented partition function that includes the new configuration, $q(N, V, T, P)$ must be modified.^{27,28} This means that in considering the augmented partition function, the addition to $q(N, V, T, P)$ —which for notational simplicity we will now denote as q_N —is not merely another q_N centered at the new location. Instead, the addition to q_N should include only new configurations in which there is at least one cluster molecule in the nonoverlapped volume du . Denoted by q_N' , the partition function of the cluster “compressed” into the lens-shaped region appearing in the figure. Since the compression is differential, q_N' clearly is given by

$$q_N' = q_N - \frac{\partial q_N}{\partial V} du \quad (10)$$

where the minus sign appears because du is positive. q_N' is the partition function of the redundant configurations so that the required addition to the partition function, less this redundancy, is $q_N - q_N'$. Substituting eq 10 into this expression gives, for the addition

$$q_N - q_N' = \frac{\partial q_N}{\partial V} du \quad (11)$$

so that the augmented partition function becomes

$$q_N + \frac{\partial q_N}{\partial V} du \quad (12)$$

We can now write

$$\frac{\partial q_N}{\partial V} = q_N \frac{\partial \ln q_N}{\partial V} = q_N \frac{P_N}{kT} = q_N \frac{P}{kT} \quad (13)$$

where the last step would be valid for an EMLD cluster. Substitution of eq 13 into eq 12 yields for the augmented partition function

$$Q_N(du) = q_N + \frac{P}{kT} q_N du \quad (14)$$

We can now repeat the cluster displacement, and some thought will show that in each displacement there will be an augmentation of the partition function exactly equal to the second term on the right in eq 14. If the process of displacement is continued until the entire volume V_{tot} is covered, the resulting partition function will then contain a sum of such terms that represents an integral over V_{tot} such that, in place of eq 14, we obtain

$$Q_N(V_{\text{tot}}) = q_N + q_N \frac{PV_{\text{tot}}}{kT} \approx q_N \frac{PV_{\text{tot}}}{kT} = \frac{PV_{\text{tot}}}{kT} q(N, P, V, T) = \Phi_N(V_{\text{tot}})q(N, V, T, P) \quad (15)$$

where in the second step we have retained only the term in V_{tot} because of its overwhelming macroscopic size. Thus

$$\Phi_N(V_{\text{tot}}) = \frac{PV_{\text{tot}}}{kT} \quad (16)$$

so that

$$Q_N(V_{\text{tot}}) = \frac{PV_{\text{tot}}}{kT} q(N, V, T, P) \quad (17)$$

6. The Equilibrium Distribution of Clusters

We shall be interested in deriving the nucleation rate via the Frenkel–Zeldovich theory.^{29,30} A prerequisite to this analysis is the evaluation of the “equilibrium distribution” of clusters. If the clusters and the surrounding supersaturated vapor are assumed to form an ideal gas mixture of molecules in which clusters are rare (as we shall assume), then in the canonical ensemble the equilibrium number of clusters containing N molecules, in a fixed volume V , is known³¹ to be

$$C_N = Q_N(V_{\text{tot}})e^{N\mu/kT} \quad (18)$$

where Q_N is the canonical ensemble partition function of the cluster and μ is the chemical potential of the vapor. Since the supersaturated gas is at constant pressure rather than constant volume, it is appropriate to ask for the corresponding formula in the isobaric–isothermal ensemble. It can be shown that a formula similar to eq 18 holds in which C_N is replaced by an average number $\langle C_N \rangle$ generated by the fact that the volume V_{tot} in the ensemble fluctuates at constant P . However, when the gas is assumed to be macroscopic, fluctuations can be neglected and the formula generated by the maximum term in the isobaric–isothermal ensemble can be used. The volume going with this maximum term can be shown to be $V_{\text{tot}}^{\text{max}} = N_{\text{tot}}kT/P$, consistent with the ideal nature of the gas, and the formula corresponding to the term is once again eq 18. Thus we shall use eq 18.

Although, eq 18 is commonly used, it is not always recognized that some clusters, by their definition, do not constitute components of an *ideal* gas mixture. This is the case of the class of clusters we have been treating, and especially of the EMLD cluster that forms a member of this class. The nonideality stems from the fact that the rigid spherical container of volume V excludes surrounding vapor molecules so that the exclusion corresponds to a nonzero intermolecular potential. Fortunately, the modification of eq 18 to take this effect into account is easy, and a simple adjustment³¹ leads to the result

$$C_N = Q_N(V_{\text{tot}}) \exp\{(N\mu - PV)/kT\} \quad (19)$$

In essence, PV represents the minimum work that must be expended in forming a cavity in the vapor large enough to accommodate the spherical shell.

Turning to the cluster, not adjusted for translation, we specify its canonical ensemble partition function q_N in some detail. First we note that the Gibbs free energy of the cluster along a constant, P, V, T path of growth can be denoted as $G(N, P, T, V)$ and that its Helmholtz free energy can then be expressed as

$$F(N, P, V, T) = G(N, P, V, T) - PV \quad (20)$$

and that the canonical ensemble partition function can be represented by the standard formula

$$q_N = q(N, P, V, T) = \exp\{-F(N, P, V, T)/kT\} = \exp\{-[G(N, P, T, V) - PV]/kT\} \quad (21)$$

Now $(\Delta G)_{\text{form}}$, the change of Gibbs free energy involved in the formation of the cluster within the supersaturated vapor of constant P is

$$(\Delta G)_{\text{form}} = G_{\text{final}}(N, P, V, T) - G_{\text{initial}}(N, P, T)$$

or

$$G_{\text{final}}(N, P, V, T) = (\Delta G)_{\text{form}} + G_{\text{initial}}(N, P, T) \quad (22)$$

where the subscripts *initial* and *final* represent the initial and final states of the N molecules. The inclusion of V as an independent variable in the initial state, in which n the number of molecules in the capillary drop is zero, would be incorrect since in that state G is fully determined by N, P, T . In any event, the initial volume is larger than V . If the capillary drop is in simple Kelvin equilibrium with its surrounding vapor, the same could be said of the final state in which n is not zero, because the Kelvin relation is an additional condition, that reduces the number of free variables; e.g., it could be regarded as determinative of n . If the Kelvin relation is not satisfied, then the

arbitrary fixing of n requires the action of some possibly complicated field in order to maintain equilibrium so that thermodynamics could apply. This additional field could itself be treated as an additional variable, but it is just as easy to regard n or V as that variable. In any event, what would have been regarded as a three-variable system in the presence of the Kelvin relation becomes a four-variable system when n is arbitrarily fixed.

Substitution of eq 22 into eq 21 yields

$$q(N, P, V, T) = \exp\{-(\Delta G)_{\text{form}} + G_{\text{initial}}(N, P, T) - PV/kT\} \quad (23)$$

But, since the initial state corresponds to a uniform density distribution at a pressure P , and chemical potential μ

$$G_{\text{initial}}(N, P, T) = N\mu \quad (24)$$

so that eq 23 becomes

$$q(N, P, V, T) = \exp\{-(\Delta G)_{\text{form}} + N\mu - PV/kT\} \quad (25)$$

and eq 17 can be written as

$$Q_N(V_{\text{tot}}) = \frac{PV_{\text{tot}}}{kT} q(N, P, V, T) = \frac{PV_{\text{tot}}}{kT} \exp\{-(\Delta G)_{\text{form}} + N\mu - PV/kT\} \quad (26)$$

Substitution of this result into eq 19 yields

$$C_N = \frac{PV_{\text{tot}}}{kT} \exp\{-(\Delta G)_{\text{form}}/kT\} \quad (27)$$

The equilibrium *concentration* of clusters is then given by

$$c_N = \frac{C_N}{V_{\text{tot}}} = \frac{P}{kT} \exp\{-(\Delta G)_{\text{form}}/kT\} \quad (28)$$

Notice that the work $(\Delta G)_{N, P, T}$ corresponds to enclosing N molecules, at uniform density, in a supersaturated vapor of pressure P in a volume large enough to accommodate them and reversibly reducing the volume to V while gathering the molecules into a state of nonuniform radial density.

7. Nucleation Rate and Zeldovich Factor

To compute the nucleation rate, we need to know the curvature at the top of the nucleation free energy barrier. We will use the simplest available theory for this purpose, one that regards N as a continuous variable. In essence we need to calculate the Zeldovich factor.³⁰

We proceed to the construction of the rate theory. Following the Frenkel-Zeldovich approach,^{29–30} we write the flux of clusters from size N to size $N + 1$, in size space, as

$$J_N = \beta_N f_N - \gamma_{N+1} f_{N+1} \quad (29)$$

where f_N is the possibly nonequilibrium concentration of clusters of size N , β_N is the number of molecules per second that hit and stick to a cluster of size N , and γ_{N+1} is the number per second that escape from a cluster of size $N + 1$.

From simple kinetic theory for impingement of molecules on a flat surface

$$\beta_N = \beta A(N) = \beta \left[4\pi \left(\frac{3v_l \Delta N}{4\pi} \right)^{2/3} \right] \quad (30)$$

where

$$\beta = P / \sqrt{2\pi m k T} \quad (30b)$$

is the kinetic theory number of molecules hitting unit area of a flat surface, $A(N)$ being the “effective” collision area and m the molecular mass of the gas. In the second equality of eq 30, it has been assumed that the effective collision area is determined by the radius of the spherical capillary drop containing a number of molecules equal to the excess ΔN of the cluster. Furthermore, in eq 30, it is assumed that the sticking coefficient is unity, i.e., it is assumed that every molecule that hits the drop is absorbed.

At equilibrium, the flux is zero, and the equilibrium cluster distribution inserted into eq 29 yields (through an application of the principle of detailed balance)

$$0 = \beta_N c_N - \gamma_{N+1} c_{N+1} \quad \text{or} \quad \gamma_{N+1} = \beta_N c_N / c_{N+1} \quad (31)$$

Substitution of this relation into eq 29 yields

$$J_N = \beta_N c_N \left[\frac{f_N}{c_N} - \frac{f_{N+1}}{c_{N+1}} \right] \quad (32)$$

Passing to the continuum, eq 32 may be expressed as

$$J(N) = -\beta(N) c(N) \left[\frac{\partial [f(N)/c(N)]}{\partial N} \right] \quad (33)$$

so that the equation describing the evolution in time of the distribution of clusters becomes

$$\frac{\partial f(N,t)}{\partial t} = - \frac{\partial J(N)}{\partial N} = \frac{\partial}{\partial N} \left(\beta(N) c(N) \left[\frac{\partial [f(N,t)/c(N)]}{\partial N} \right] \right) \quad (33b)$$

which has the form of a Fokker–Planck equation.

The nucleation rate J is conventionally defined as the flux of eq 33, at $N = N^*$ where N^* is the size of the nucleus. The following approximate (but physically reasonable) boundary conditions are conventionally applied to eq 33.

$$f/c \rightarrow 1, N \rightarrow 0 \quad \text{and} \quad f/c \rightarrow 0, N \rightarrow \infty \quad (34)$$

Rearranging eq 33 and integrating with respect to N gives

$$\int_0^\infty \frac{J(N) dN}{\beta(N) c(N)} = \left(\frac{f}{c} \right)_{N=0} - \left(\frac{f}{c} \right)_{N=\infty} = 1 \quad (35)$$

where eq 34 has been used. The sharp maximum of $[\beta(N) c(N)]^{-1}$ at N^* ³² allows eq 35 to be approximated by

$$J = J(N^*) = \frac{1}{\int_0^\infty \frac{dN}{\beta(N) c(N)}} \quad (36)$$

To proceed further we integrate the previous equation using the steepest descents approximation, by expanding $(\Delta G)_{\text{form}}$ in $c(N)$ about N^* , keeping the quadratic term, and performing the subsequent Gaussian integration. In the expansion

$$\left\{ \frac{\partial (\Delta G)_{N,P,T}}{\partial N} \right\}_{N=N^*} = 0 \quad (37)$$

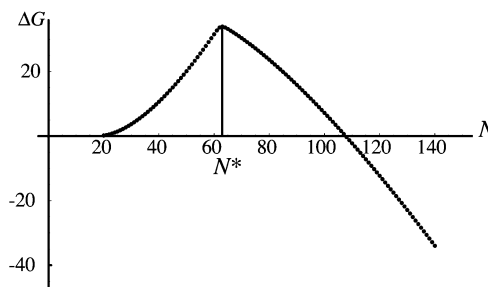


Figure 5. Plot of $(\Delta G)_{\text{form}}$ vs N at $T = 241.81$ K and $S = 172$. The plot peaks at the critical cluster size $N^* = 63$.

The final result for the nucleation rate is

$$J = \beta(N^*) \left(\frac{P(N)}{kT} \right) \left[\frac{1}{2\pi kT} \left| \frac{\partial^2 (\Delta G)_{N,P,T}}{\partial N^2} \right|_{N=N^*} \right]^{1/2} \exp\{-(\Delta G^*_{\text{form}})/kT\} \quad (38)$$

In this expression the quantities involving $(\Delta G)_{\text{form}}$ are available from eqs 1 and 3. The Zeldovich factor is automatically contained in the preexponential factor of eq 38.

8. Nucleation Rate of 1-Pentanol

In this section, we apply the theory developed in previous sections to evaluate the rate of nucleation at different temperatures and supersaturations for 1-pentanol. The choice of 1-pentanol stems from the presence of abundant experimental data on this substance. In 1995 1-pentanol was selected by the nucleation community as the target compound on which to perform a series of experiments on homogeneous nucleation. The experiments were performed over as wide a range of nucleation rates as possible using all available techniques.

The ingredients required to evaluate nucleation rates according to eq 38 are the height of the nucleation barrier, the Zeldovich factor, and the rate of attachment of molecules to the critical cluster. All these quantities can be now evaluated from EMLD-DNT.

As noted in the Introduction, the EMLD-DNT model, and in particular eq 3, provides the tool for the evaluation of $(\Delta G^*)_{\text{form}}$ the height of the nucleation barrier for any value of the pressure P , or equivalently, the supersaturation. More specifically, at a given pressure P and temperature T of interest, using EMLD-DNT we can calculate the size N^* of the critical nucleus and volume V^* , at the minimum of the pressure–volume isotherm for N^* , that correspond to that pressure P . Then, knowing N^* and V^* , $(\Delta G^*)_{\text{form}}$ can be readily evaluated using eq 3.

The Zeldovich factor, the quantity in the square brackets in eq 38, can also be calculated numerically by finding the second derivative with respect to N , at $N = N^*$ of $(\Delta G)_{\text{form}}$ given by eq 7. Following our discussion of the growth path in section 4, we evaluate the Zeldovich factor along a constant P, V, T path. Figure 5 illustrates an example of the shape of $(\Delta G)_{\text{form}}$ vs N for fixed values of P^*, V^*, T . The figure shows that $(\Delta G)_{\text{form}}$ peaks at N^* , the critical nucleus size, as expected. Finally, the last quantity we need, namely, the rate of attachment β in eq 38, can be evaluated according to eqs 30 and 30b, using the excess ΔN^* obtained from the nucleation theorem eq 5. We are now ready to compare the predictions for the rate of nucleation given by EMLD-DNT with the experimental results.

Figure 6 compares the predictions of the EMLD-DNT with the experiments performed in 1996 (triangles)²⁰ and 2004 (circles)¹⁹ in a nucleation pulse chamber by Strey's group. To evaluate the rates, we have used the macroscopic thermophysical

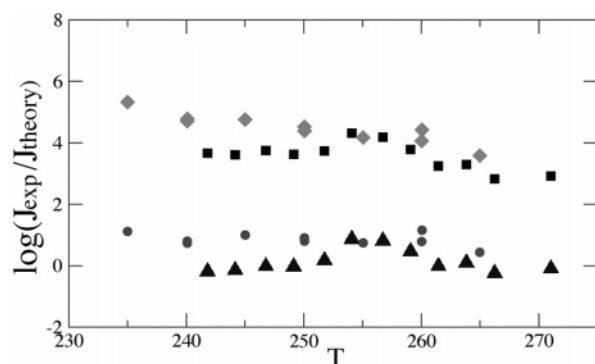


Figure 6. Comparison of our theoretical results for the nucleation rate of 1-pentanol with the experimental data of ref 20 (triangles and circles) and the predictions of CNT (squares and diamonds). The actual data are presented in Tables 2 and 3.

TABLE 1: Thermophysical Properties of 1-Pentanol^a

$M = 88.15$	g mol^{-1}
$t = T - 273.15$	
$\sigma = 0.02678 - 8.147 \times 10^{-5}t$	N m^{-1}
$P_{\text{eq}} = 133.324 \exp(90.08 - 9788/T - 9.90 \ln T)$	Pa

^a The properties are M , the molecular weight; P_{eq} , equilibrium vapor pressure; T , temperature in kelvin; ρ_l , liquid density; σ , surface tension.

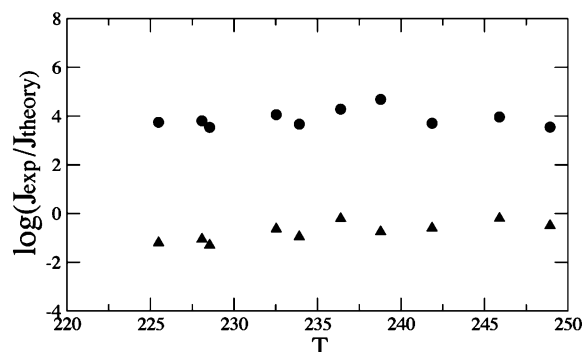


Figure 7. Comparison of the experimental nucleation rates of ref 18 with the results of EMLD-DNT (triangles) and CNT (circles). The actual data are presented in Table 4.

properties listed in Table 1. The experimental nucleation rate is $10^7 \text{ cm}^{-3} \text{ s}^{-1}$ in all cases presented in the figure. The squares and diamonds illustrate the predictions of CNT, which are about 4 orders of magnitude smaller than the experimental results. The triangles and circles correspond to the predictions of EMLD-DNT. In the majority of cases, the nucleation rates obtained by our theory vary by a factor of about 2 from the experimental data of 1996 (triangles) and a factor of about 6 from that of 2004 (circles) (see Figures 2 and 3 in Appendix B). Considering the difficulties and the uncertainty involved in experimental measurements of nucleation rates, and in the thermophysical properties of the substance (specially in the surface tension), our theory seems to be in excellent agreement with experiment.

It is obvious that one cannot expect such an almost perfect agreement between the predictions of the theory and the experimental data for the whole range of supersaturations and temperatures. For example, at high supersaturations the non-ideality of the supersaturated vapor may start to play an important role in the nucleation process, which could result in deviations between our simple theory and experiments.

Figure 7 compares the predictions of the EMLD-DNT model with experiments performed in a higher range of supersaturation, achieved by using a supersonic nozzle.¹⁸ In those experiments, the nucleation rate J was estimated to be in the range of $2 \times$

$10^{16} < J < 10^{17}$ and corresponded to measured supersaturations in the range of 40–177. We have assumed that $J_{\text{exp}} = 10^{17}$ to calculate the data presented in Figure 7. Note that in this case our results overestimate the experimental nucleation rates by about 1 order of magnitude, specially at low temperatures and high supersaturations. This discrepancy is reasonable and could be expected on the basis of the simplifications of the model and the new physical ingredients that may start to play a role at such conditions. As part of the nonideality of the vapor phase, effects, such as the association of dimers,^{33,34} can increase the stability of the supersaturated vapor and reduce the experimental nucleation rates. Additionally, at the very high supersaturations achieved in supersonic nozzle experiments, the height of nucleation barrier is rather low (less than $10 k_B T$) and some of the approximations involved in the evaluation of the nucleation rate can lose their validity. Still it is important to note that the results of our model are reasonably accurate and much better than those of CNT, which predicts a nucleation rate which is about 4 orders of magnitude smaller than the experimental data.

9. Conclusion

In summary, we have formulated a quantitative theory for the evaluation of the nucleation rate according to the EMLD-DNT model. We have developed a theory for the rate that is consistent with that model and which includes properly the contributions of translation, the kinetics of attachment of molecules, and the so-called Zeldovich factor. We have found that the resulting prefactor is typically a factor of 3–5 larger than that of the CNT.

We have then applied the new theory to the nucleation of 1-pentanol and obtained excellent agreement with experiment. The distinguishing feature of our theory is that it uses only the macroscopic thermophysical parameters of nucleating systems and does not depend on the intermolecular potential of specific substances. Therefore, with the sole knowledge of the values of these macroscopic observables, i.e., using the same ingredients as CNT, we are able to evaluate both the height of the nucleation barrier and the nucleation rate. And for the case of pentanol, we have, indeed, found a remarkable agreement between theory and experiment.^{18–20}

Some words about the importance of the preexponential factor in the expression for the rate of nucleation are appropriate. In several recent non-CNT publications the preexponential factor appearing in CNT has been used, once the exponential factor has been evaluated, thus avoiding some difficult theory. The rationale behind this approach is that the preexponential factor is not very sensitive to supersaturation and, in any case, could easily be estimated to within an order of magnitude by almost any crude theory. Indeed, this conclusion has been supported by some simulation.³⁵ However, it should be borne in mind that accuracy to within an order of magnitude is acceptable as long as experiments are only accurate to within the same degree. When they become more accurate, a theory of the preexponential factor will have to be improved accordingly. At the moment, a theory that includes only a crude estimate of the factor is suitable for predicting onset supersaturations, but one should not become too comfortable with the idea that more sophisticated theories of the factor are not necessary. Indeed, simulation of an unlimited multitude of substances and comparison with CNT might reveal some cases in which the use of the CNT preexponential factor does not provide an equally accurate estimate.

In the present paper, our theory of the preexponential factor is crude, but it does involve an improvement over previous theories

in that it includes effects due, for example, to cluster translation and the “exclusion volume” of a cluster—effects that CNT ignores. A focus on these effects represents a first step in a possibly more refined theory. We also note that it is the need to deal with the preexponential factor that gives rise to the need to determine the “growth path” on the free energy landscape as we have. In any event, the theory of this factor should be consistent with that for the determination of the free energy barrier—again an approach adopted in the present work. In this connection it should be noted that the use of the CNT preexponential factor as discussed above assumes that the growth flux on the free energy landscape is one-dimensional even though the landscape itself is two-dimensional (N, V). Our careful treatment of the preexponential factor provides the precise argument for the choice of one-dimensional “growth path”.

The theory developed in this paper can be applied to any system, although its application to more complicated substances must be done with some care. Effects, such as the nonideality of the vapor phase, the heat of association, or the Tolman length, are ignored in the present work. These are potentially important factors in the evaluation of nucleation rates and we will take them into account in a future work.

Acknowledgment. It is a pleasure to dedicate this theory to Charles Knobler, whose seminal work in so many areas of physical chemistry including nucleation has taught many of us so much. This work has been supported by the National Science Foundation under NSF Grant No. CHE-03013563. D.R. acknowledges support by the Ministerio de Ciencia y Tecnología of Spain through the “Ramón y Cajal” program.

Appendix A: Proof of Equation 3

In this Appendix we present the derivation of eq 3. Note that the basic idea underlying the EMLD-DNT model is to obtain an accurate estimate of $(\Delta G)_{\text{form}}$ or $\Delta\Omega$ (the relevant work of nucleus formation) from the value of ΔF , which is the equilibrium Helmholtz free energy of an (N, V, T) system minus the hypothetical Helmholtz free energy of a homogeneous supersaturated vapor consisting of N molecules confined to a volume V at a temperature T . Both the homogeneous vapor (state 1) and the cluster (state 2) have the same values of (N, V, T), but they have different values of pressure!! The pressure of the equilibrium (N, V, T) cluster is P while that of the homogeneous vapor is $P_0 = NkT/V$ (assuming an ideal gas). Therefore, we have

$$\Delta F = F_2(N, V, T; P, \mu) - F_1(N, V, T; P_0, \mu_0)$$

where μ_0 is the chemical potential of the homogeneous vapor. Note that the variables N , V , and T are the same in the initial and final states; however, pressures are not the same. In general, the work of formation of a cluster along a particular path is always equal to the increase of the thermodynamic potential characteristic of that path. Thus, the work of formation of a cluster along a path of (μ, V, T) is given by the change in the grand potential as follows

$$\Delta\Omega = \Omega_2(\mu, V, T; N, P) - \Omega_1(\mu, V, T; N', P)$$

While the variables (μ, V, T) are the same in the initial and final states, N is changed. Similarly, to calculate the increase in the Gibbs free energy along an (N, P, T) path, $\Delta G = \Delta G_2(N, P, T; V, \mu) - \Delta G_1(N, P, T; V', \mu)$, the initial values of (N, P, T) are the same as the final ones, but the volume of the system

TABLE 2: Experimental Data Are Taken from Ref 20^a

temp (K)	supersaturation	experimental rate (cm ⁻³ s ⁻¹)	classical nucleation rate (cm ⁻³ s ⁻¹)	EMLD-DNT rate (cm ⁻³ s ⁻¹)
241.81	17.2	10 ⁷	2155	1.55 × 10 ⁷
244.16	16	10 ⁷	2469	1.40 × 10 ⁷
246.77	14.6	10 ⁷	1795	1.06 × 10 ⁷
249.14	13.7	10 ⁷	2362	1.07 × 10 ⁷
251.76	12.6	10 ⁷	1825	6.76 × 10 ⁶
254.09	11.4	10 ⁷	486	1.36 × 10 ⁶
256.74	10.7	10 ⁷	651	1.54 × 10 ⁶
259.09	10.3	10 ⁷	1640	3.43 × 10 ⁶
261.46	10.0	10 ⁷	5684	1.04 × 10 ⁷
263.84	9.4	10 ⁷	5114	0.80 × 10 ⁷
266.24	9.1	10 ⁷	14934	2.10 × 10 ⁷
268.62	8.6	10 ⁷	14837	1.76 × 10 ⁷
271.03	8.1	10 ⁷	12092	1.26 × 10 ⁷

^a Nucleation rate is evaluated based on eq 38.

TABLE 3: Experimental Data Are Taken from Ref 19^a

temp (K)	supersaturation	experimental rate (cm ⁻³ s ⁻¹)	classical nucleation rate (cm ⁻³ s ⁻¹)	EMLD-DNT rate (cm ⁻³ s ⁻¹)
250.05	12.6	10 ⁷	302.69	1.25 × 10 ⁶
264.98	9.0	10 ⁷	2611.72	3.71 × 10 ⁶
260.03	9.9	10 ⁷	863.52	1.63 × 10 ⁶
255.05	11.2	10 ⁷	670.88	1.80 × 10 ⁶
245.01	14.4	10 ⁷	173.79	1.01 × 10 ⁶
240.08	16.9	10 ⁷	198.19	1.85 × 10 ⁶
235.00	19.2	10 ⁷	47.35	0.77 × 10 ⁶
260.06	9.7	10 ⁷	377.36	0.70 × 10 ⁶
250.07	12.7	10 ⁷	414.79	1.59 × 10 ⁶
240.09	16.8	10 ⁷	164.89	1.59 × 10 ⁶

^a Nucleation rate is evaluated based on eq 38.

TABLE 4: Experimental Data Are Taken from Ref 18^a

temp (K)	supersaturation	experimental rate (cm ⁻³ s ⁻¹)	classical nucleation rate (cm ⁻³ s ⁻¹)	EMLD-DNT rate (cm ⁻³ s ⁻¹)
248.93	40	10 ¹⁷	2.81 × 10 ¹³	3.12 × 10 ¹⁷
245.9	43	10 ¹⁷	1.08 × 10 ¹³	1.58 × 10 ¹⁷
241.86	55	10 ¹⁷	1.97 × 10 ¹³	3.95 × 10 ¹⁷
238.78	65	10 ¹⁷	2.06 × 10 ¹²	5.59 × 10 ¹⁷
236.39	66	10 ¹⁷	5.20 × 10 ¹²	1.61 × 10 ¹⁷
233.91	86	10 ¹⁷	2.13 × 10 ¹³	8.98 × 10 ¹⁷
232.53	86	10 ¹⁷	8.69 × 10 ¹²	4.28 × 10 ¹⁷
228.08	120	10 ¹⁷	1.56 × 10 ¹³	1.13 × 10 ¹⁸
228.54	124	10 ¹⁷	2.90 × 10 ¹³	1.99 × 10 ¹⁸
225.48	145	10 ¹⁷	1.80 × 10 ¹³	1.58 × 10 ¹⁸
222.79	177	10 ¹⁷	1.96 × 10 ¹³	2.24 × 10 ¹⁸

^a Nucleation rate is evaluated based on eq 38.

changes. Note that in all the noted cases, the initial states are not the same; however, they allow the same final states to be reached via the respective (N, P, T) , (μ, V, T) , and (N, V, T) processes.

One can now easily obtain $(\Delta G)_{\text{form}}$ or $\Delta\Omega$, as follows

$$G_2(N, P, T; V, \mu) = F_2(N, V, T; P, \mu) + PV$$

or

$$G_2(N, P, T; V, \mu) = [F_2(N, V, T; P, \mu) - N\mu] - (-PV) + N\mu = \Omega_2(\mu, V, T; N, P) - \Omega_1(\mu, V, T; N', P) + G_1(N, P, T; \mu, V)$$

where primed quantities refer to state 1. Therefore

$$\Delta G = \Delta\Omega$$

The relation between $\Delta\Omega$ and ΔF obtained in eq 3 can also be easily derived as follows

$$\begin{aligned}\Delta F &= F_2(N, V, T; \mu, P) - F_1(N, V, T; \mu_0, p_0) = \\ &[\Omega_2(\mu, V, T; N, P) + N\mu] - F_1(N, V, T; \mu_0, p_0) = \\ &[\Omega_2(\mu, V, T; N, P) + PV] + N\mu - F_1(N, V, T; \mu_0, p_0) - PV = \\ &[\Omega_2(\mu, V, T; N, P) - \Omega_1(\mu, V, T; N', P)] + N\mu - [N\mu_0 - p_0V] - \\ &PV = \Delta\Omega + N(\mu - \mu_0) - V(P - p_0)\end{aligned}$$

Appendix B: Tables

The results for 1-pentanol plotted in Figures 6 and 7 are given in Tables 2-4.

References and Notes

- (1) Abraham, F. F. *Homogeneous Nucleation Theory*; Academic Press: New York, 1974.
- (2) Laaksonen, A.; Talanquer, V.; Oxtoby, D. W. *Annu. Rev. Phys. Chem.* **1995**, *46*, 489.
- (3) Wilemski, G. *J. Chem. Phys.* **1984**, *80*, 1370.
- (4) Wilemski, G. *J. Chem. Phys.* **1987**, *91*, 2492.
- (5) Dillmann, A.; Meier, G. E. A. *Chem. Phys. Lett.* **1989**, *160*, 71; *J. Chem. Phys.* **1991**, *94*, 3872.
- (6) Kalikmanov, V. I.; van Dongen, M. E. H. *Phys. Rev. E* **1993**, *47*, 3532; *J. Chem. Phys.* **1995**, *103*, 4250.
- (7) Talanquer, V. *J. Chem. Phys.* **1997**, *106*, 9957.
- (8) Kashchiev, D. *J. Chem. Phys.* **2003**, *118*, 1837.
- (9) Schmelzer, J. W. P.; Schmelzer, J.; Gutzow, I. S. *J. Chem. Phys.* **2000**, *112*, 3820.
- (10) Moody, M. P.; Attard, P. *Phys. Rev. Lett.* **2003**, *91*, 056104.
- (11) Reguera, D.; Bowles, R. K.; Djikaev, Y.; Reiss, H. *J. Chem. Phys.* **2003**, *118*, 340.
- (12) Reguera, D.; Reiss, H. *J. Chem. Phys.* **2003**, *119*, 1533.
- (13) Reiss, H.; Reguera, D. *J. Phys. Chem. B* **2004**, *108*, 6555.
- (14) Schenter, G. K.; Kathmann, S. M.; Garrett, B. C. *Phys. Rev. Lett.* **1999**, *82*, 3484.
- (15) Schenter, G. K.; Kathmann, S. M.; Garret, B. C. *J. Chem. Phys.* **1999**, *110*, 7951.
- (16) Reguera, D.; Reiss, H. *J. Phys. Chem. B* **2004**, *108*, 19831.
- (17) Reguera, D.; Reiss, H. *Phys. Rev. Lett.* **2004**, *93*, 165701.
- (18) Gharibeh, M.; Kim, Y.; Dieregswiler, U.; Wyslouzil, B. E.; Ghosh, D.; Strey, R. *J. Chem. Phys.* **2005**, *122*, 094512.
- (19) Iland, K.; Wedkind, J.; Wolk, J.; Wanger, P. E.; Strey, R. *J. Chem. Phys.* **2004**, *121*, 12259.
- (20) Hruby, J.; Viisanen, Y.; Strey, R. *J. Chem. Phys.* **1996**, *104*, 5181.
- (21) Ten Wolde, P. R.; Frenkel, D. *J. Chem. Phys.* **1998**, *109*, 9901.
- (22) Lee, D. J.; Telo da Gama, M. M.; Gubbins, K. E. *J. Chem. Phys.* **1986**, *85*, 490.
- (23) Kashchiev, D. *J. Chem. Phys.* **1982**, *76*, 5098.
- (24) Bowles, R. K.; Reguera, D.; Djikaev, Y.; Reiss, H. *J. Chem. Phys.* **2001**, *115*, 1853; *ibid* **2002**, *116*, 2330.
- (25) Reiss, H. *J. Stat. Phys.* **1970**, *2*, 83.
- (26) Talanquer, V.; Oxtoby, D. W. *J. Chem. Phys.* **1994**, *100*, 5190.
- (27) Reiss, H.; Kegel, W. K.; Katz, J. L. *J. Phys. Chem. A* **1998**, *102*, 8548-8555.
- (28) Burton, J. J. *Statistical Mechanics, Part A: Equilibrium Techniques, Modern Theoretical Chemistry*; Plenum: New York, 1977; Vol. 5, p 195.
- (29) Frenkel, J. *J. Chem. Phys.* **1939**, *7*, 200.
- (30) Zeldovich, Y. B. *Zh. Eksp. Teor. Fiz.* **1942**, *12*, 525.
- (31) Reiss, H.; Bowles, R. K. *J. Chem. Phys.* **1999**, *111*, 7501.
- (32) Cohen, E. R. *J. Stat. Phys.* **1970**, *2*, 147.
- (33) Katz, H. L.; Saltsburg, H.; Reiss, H. *J. Colloid Interface Sci.* **1966**, *21*, 560.
- (34) Heist, R. H.; Janjua, M.; Ahmed, J. *J. Chem. Phys.* **1994**, *98*, 4443.
- (35) Auer, S.; Frenkel, D. *Adv. Polym. Sci.* **2005**, *173*, 149.